Tensile Capacity of Spliced GFRP Bars using Filled Hollow GFRP Sleeves

Taha Eldaleel, Fareed Elgabbas, Khalid M. Morsy, Ahmad F. Abdelaziz

Abstract— The main goal of this research is to develop an alternative method to connect precast concrete elements reinforced with GFRP bars using GFRP sleeves to minimize connection length and improve corrosion resistance. To investigate the tensile capacity of GFRP sleeve splice bars, six specimens were tested under tension load up to failure according to ASTM D7205 [1]. Two variables were considered in this study: (i) Embedment length of the GFRP bar in the splice sleeve (13.75- and 16.25-times bar diameter), (ii) Number of GFRP layers wrapping the sleeve in the radial direction (No wrap, two layers, and four layers). The test results show that the tensile capacity increased by increasing sleeve radial confinement using external GFRP wrapping, as well as bar embedment length. Thus, an aqueduct radial stiffness and bar embedment length are required to achieve bar tensile strength.

INDEX TERMS— GFRP Bars, Precast structural joints, Sleeve connector, GFRP sleeve.

1. INTRODUCTION

Recently, precast concrete technology has found its way in a lot of commercial and residential construction projects because of its significant advantages compared to cast in situ constructions. It causes a reduction in the overall cost of the structure since it reduced the project duration as the erection processes are unaffected by the great variation in the productivity of laborers and weather fluctuations. Also, using the precast elements leads to less waste material, reduction in in-situ labor and workforce, as well as reduction in formwork in the site led to reduced overall construction cost. Besides, it provides high-quality control as it produced in precast producers' plants using high-tech machinery in ideal labor conditions [2]. Furthermore, other significant advantages are achieved by precast constructions such as improved modularization and standardization of components compared to components produced in-situ [3], provide better architectural appearance [4], [5], improving durability, higher flexibility in design, less impact on the environment, better occupational health and safety, and enhancing sustainability e.g.[2]–[4], [6]–[8]. However, the connections between precast elements are the main problem that faces precast technology and restricted using precast elements as a continuous element. Moreover, the traditional connection between precast elements that use lap-splice connection led to making the connection length larger and complicated.

Thus, several studies proposed using grouted splice sleeve to connect reinforced bars for easier and faster construction, as well as minimizing connection length. Various splice sleeve shapes were investigated to increase bond strength by increasing confinement pressure such as welded steel bar [9], square ribbed hollow section [10], high strength bolts [11], steel pipes with spiral steel [9], and sleeves with tapered shape [12]. Moreover, some researchers investigate different sleeve materials to avoid corrosion problems such as glass fiber reinforced polymers [13]–[16].

In this experimental study, an alternative proposal to connect precast elements was investigated by using a durable GFRP sleeve filled with epoxy in order to avoid corrosion problems and make the connection smaller for faster and easier construction. This research investigates the optimum embedment length in a GFRP sleeve filled with epoxy to achieve the bar tensile strength taken into consideration the effect of radiale confinement using GFRP layers.

2. EXPERIMENTAL PROGRAM

2.1 Material Properties

Glass-fiber-reinforced polymer (GFRP) bars of 12 mm diameter with a deformed surface with helical ribs were used in this study. Moreover, the fabricated sleeves were fabricated using GFRP sheets (SikaWrap-430 G), as shown in Figure 1. The GFRP sheet consisted of unidirectional glass fiber fabric roving. The fiber type was E-glass fiber, while dry fiber thickness was 0.168 mm which is based on total glass content. The properties of the fabric, the cured laminates, and the epoxy adhesive are listed in Table 1. GFRP sheets were used to fabricate GFRP sleeves by wrapping the sheet on PVC tubes in an axial direction and then wrapping the GFRP sleeves in the radial direction for confinement. Epoxy resin of Sikadur-31 CF was used in the GFRP sleeve coupler to splice the bars together.

1 *M.Sc. candidate Taha Eldaleel, Structural Engineering Department, Faculty of Engineering, Ain shams University, Egypt. E-mail: taha.hassan@eng.asu.edu.eg*
2 *Assistant Professor Fareed Elgabbas, Structural Engineering Department, Faculty of Engineering, Ain shams University, Egypt. E-mail: Fareed.Elgabbas@eng.asu.edu.eg*
3 *Associate Professor Khalid M. Morsy, Structural Engineering Department, Faculty of Engineering, Ain shams University, Egypt. E-mail: khalid.morsy@eng.asu.edu.eg*
4 *Associate Professor Ahmed F. Abdelaziz, Structural Engineering Department, Faculty of Engineering, Ain shams University, Egypt. E-mail: ahmed_abdelaziz@eng.asu.edu.eg*

Table 1: Properties of GFRP Wrapping System

Property	SikaWrap-430 G		Sikadur-330 Epoxy adhesive
	Fiber properties	Cured laminates	
Tensile strength (MPa)	2500	1200	30
Tensile modulus (GPa)	72	68	4.5
Elongation (%)	2.7	2.14	0.9
Density (g/cm^3)	2.56	--	--
Thickness (mm)	--	0.168	--

Note: All data was supplied by the manufacture.

Figure 1: Woven Unidirectional GFRP Sheet

2.2 Test Specimens

The experimental program consisted of two stages. **Stage I** for the control specimens which is consisted of five representative GFRP bars of 12 mm diameter and tested under static tension load according to ASTM D7205 [1]. The total length of the specimen was 1000 mm with a free length of 400 mm. The specimens' ends were anchored with a 300 mm steel tube filled with epoxy resin to be able to grip the specimen in the tension machine. Two dial gauges of a 200 mm gauge length were attached to the specimen to measure elongation. Figure 2 shows a schematic sketch of the tested specimens. **Stage II** for the spliced specimens which is consisted of six specimens made from GFRP bars and jointed together using a filled GFRP hollow sleeve. Specimens were tested under tension up to failure. All GFRP sleeves were fabricated by wrapping a 500 mm length GFRP sheet in an axial direction and then wrapping the GFRP sleeve in the radial direction for confinement. Two parameters were investigated: (i) Embedment length of the GFRP bar in the splice sleeve (13.75- and 16.25-times bar diameter), (ii) Number of GFRP layers wrapping the GFRP sleeve in the radial direction (No wrap, two layers, and four layers). Table 2 presents the details of the tested specimens. While typical specimen for GFRP sleeve connectors is shown in Figure 3.

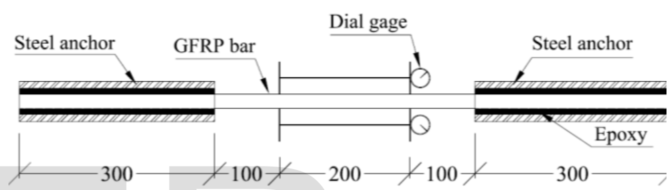

Figure 2: A Schematic Sketch for Control Tension Specimens

Figure 3: Typical Specimen for GFRP Sleeve Connectors

Table 2: The Details of Tested Spliced Specimens

Specimen ID [a]	d_b (mm)	L_d[b] (mm)	Sleeve length (mm)	GFRP wrap length (mm)	Sleeve inner diameter (mm)	sleeve outer diameter (mm)
G12-NW-13.75	12	165	330	N/A	18	26
G12-2W-13.75		165	330	175		27
G12-4W-13.75		165	330	300		28
G12-NW-16.25		195	390	N/A		26
G12-2W-16.25		195	390	175		27
G12-4W-16.25		195	390	300		28

[a] 1st segment refers to spliced bars type (G: GFRP bars), and spliced bars diameter in mm, 2nd segment refers to number of GFRP wrapping layers (NW: No wrapping, 2W: Wrapped using two layers, and 4W: Wrapped using four layers), and 3th segment refers to the embedment length as a function of bar diameters (13.75- and 16.25-times bar diameter)

[b] Embedment length of the GFRP bar inside the GFRP sleeve

2.3 Test Setup and Procedures

All control specimens were tested under static tension load up to failure, according to ASTM D7205 [1], using a universal

ISSN 2229-5518

testing machine of capacity 200 kN, as shown in Figure 4. The maximum failure load was observed while the modulus of elasticity and the ultimate strain were estimated using two dial gauges of a 200 mm gauge length. For spliced GFRP specimens, each specimen was fabricated by splicing two GFRP bars, with a length of 500 mm, end-to-end in a GFRP sleeve filled with epoxy resin. The other ends of the GFRP bars were anchored with 300 mm steel tubes length and filled with epoxy to be able to grip the specimen in the tension machine without crushing the GFRP bars due to gripping pressure. All specimen were tested under tension load up to failure according to ASTM D7205 [1]. Figure 5 shows a schematic drawing of the test setup. While Figure 6 provides a photo of the test setup for specimens. The maximum failure load and the mode of failure were observed for each specimen.

Figure 4: Test Setup for Control Specimens Tensile Test

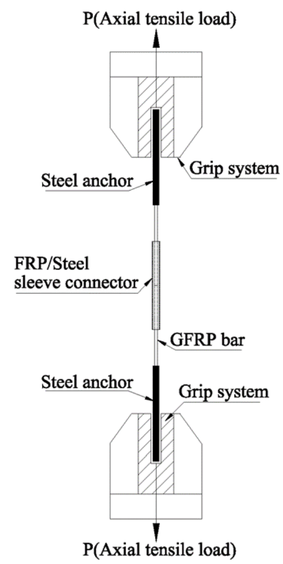

Figure 5: Scheme of Splice GFRP Specimens Tension Test

Figure 6:Test Setup for Splice GFRP Specimens Tension Test

3. Test Results and Discussions

3.1 Control GFRP Specimens (Stage I)

Five representative GFRP bars specimens of 12 mm diameter without splice were tested under static tension load, according to ASTM D7205 [1]. All control specimens, without splice, exhibited linear stress-strain relationships and failed due to rupture of fibers, as shown in Figure 7. The nominal cross-section area used to determine the tensile properties of GFRP bars were 113 mm² for 12 mm bar diameter. The mean tensile strength, modulus of elasticity, and ultimate strain of tested bars were 1081 MPa, 46.73 GPa,

ISSN 2229-5518

and 2.31%, respectively. Table 3 provides the tensile properties of the GFRP bars in detail. While Figure 8 shows the stress-strain curve for control GFRP bars.

Figure 7: GFRP Bars Tensile Failure

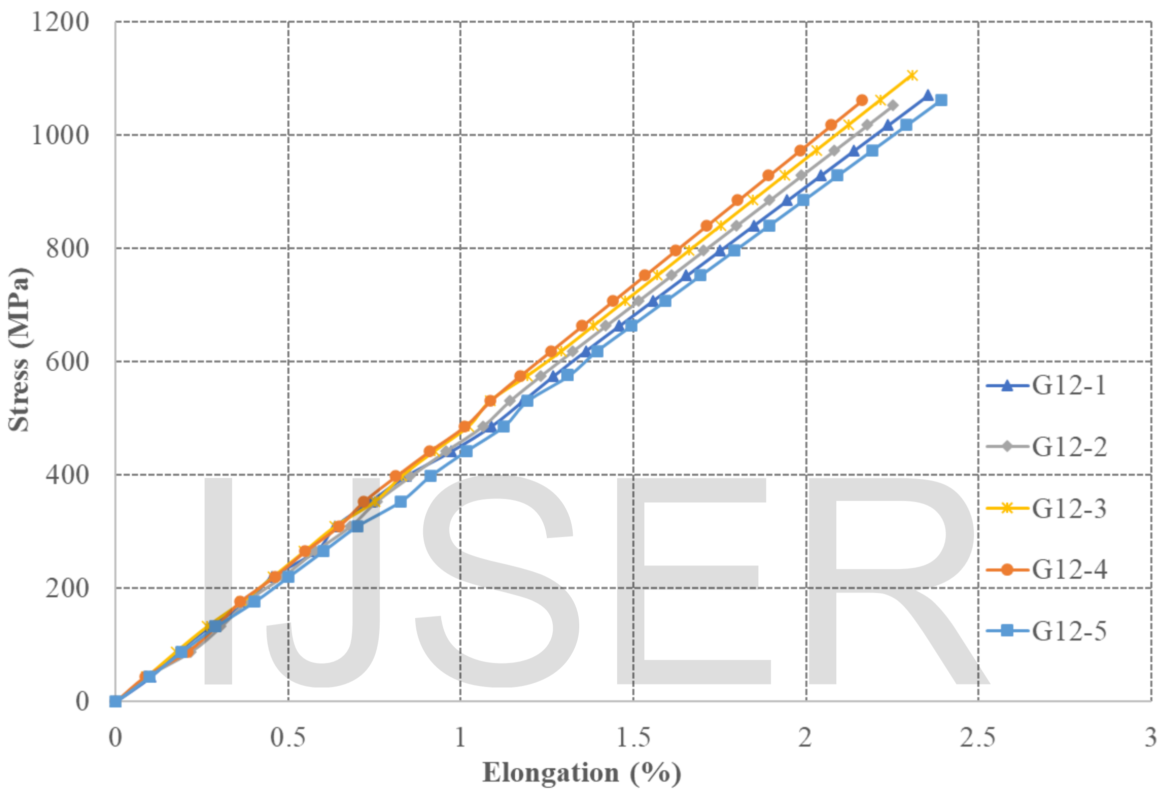

Figure 8: The Stress-Strain Curve for Control GFRP Bars

Table 3: Tensile Properties of The Control GFRP Bars

Code	Bar Diameter (mm)	Tensile Strength, f_u (MPa)	Modulus of Elasticity, E_f (GPa)	Ultimate Strain, ε_{fu} (%)
G12-1		1070.4	45.09	2.35
G12-2		1052.7	46.99	2.25
G12-3		1105.8	47.77	2.31
G12-4	12	1114.6	49.36	2.27
G12-5		1061.6	44.45	2.39
Mean Value		1081.0	46.73	2.31
Standard deviation (SD)		27.55	2.00	0.06
Coefficient of variation (CV)		2.55	4.27	2.48

3.2 Splice GFRP Specimens (Stage II)

Table 4 summarized failure loads and mode of failure for all spliced GFRP specimens. Specimen G12-NW-13.75, which consisted of two GFRP bars and spliced together using a GFRP sleeve filled with epoxy resin and has an embedment length of 13.75 times bar diameter without radial wrapping, was failed at 62 kN due to bar slippage after sleeve cracking, as shown in Figure 9. The tensile capacity of this specimen was about 50.7% of bar tensile strength. Sleeve cracking failure mode indicated that the radial stiffness of the GFRP sleeve is inadequate and failure is not controlled by bond strength yet. While specimen G12-2W-13.75, which has higher radial stiffness of the GFRP sleeve by wrapping the sleeve with two layers of GFRP sheets using the same embedment length, was failed at a load of 66 kN with the same mode of failure as specimen G12-NW-13.75. Therefore, the sleeve wrapping using two layers of GFRP sheets has a slight effect on the tensile capacity, where the tensile capacity was increased by 6% compared to specimen G12-NW-13.75 and achieved only 54.1% of bar tensile strength. In addition, wrapping the sleeve using four layers of GFRP sheets, as per specimen G12-4W-13.75, was significantly increased the tensile capacity to 72 kN. However, the specimen was failed due to bar slippage after sleeve cracking. Consequently, wrapping the sleeve using four layers of GFRP sheet increased tensile capacity by 16% compared to G12-NW-13.75 and achieved only 58.9% of bar tensile strength. Therefore, increasing radial stiffness of GFRP sleeves led to increasing spliced bars tensile capacity.

Figure 9: Failure Mode of G12-NW-13.75 (Sleeve Cracking)

However, The tensile capacity of G12-4W-13.75 still so far from the required bar tensile strength. Thus, additional specimens were fabricated similar to previous specimens after increasing the embedment length to 16.25 times bar diameter to increase bond capacity and tensile capacity. Specimen G12-NW-16.25, which has higher embedment length of 16.25 times bar diameter without radial wrapping, was failed at a load of 80 kN due to bar slippage after sleeve cracking, as shown in Figure 10. Therefore, increasing embedment length from 13.75 to 16.25 times bar diameter has a significant effect on the tensile capacity, where the tensile capacity was increased by 29% compared to specimen G12-NW-13.75 and achieved only 65.5% of bar tensile strength. While specimen G12-2W-16.25 that has higher GFRP sleeve radial stiffness by wrapping the GFRP sleeve with two GFRP layers using the same embedment length of 16.25 times bar diameter was failed at a load of 85 kN with the same mode of failure of specimen G12-NW-16.25, where the tensile capacity was increased by 6% compared to specimen G12-NW-16.25 and by 37% compared to specimen G12-NW-13.75, as well as achieved only 69.6% of bar tensile strength. Moreover, specimen G12-4W-16.25 that wrapped with four layers of GFRP sheets, was failed at 92 kN with capacity enhancement of 15% compared to specimen G12-NW-16.25 and by 48% compared to specimen G12-NW-13.75. Finally, the maximum tensile capacity achieved from this experimental work was 75% of the mean bar tensile strength by G12-4W-16.25. Besides, failure mode still affected by radial stiffness, and specimens failed due to sleeve cracking. Therefore, the test results indicated that to achieve the required bar tensile strength, adequate radial stiffness should be provided to prevent the sleeve from cracking and adequate embedment length to prevent failure accrued due to bar slippage controlled by bond stress capacity. Consequently, future studies are needed to fabricate GFRP sleeves in plants with an adequate radial stiffness.

Figure 10: Failure Mode of G12-NW-16.25 (Sleeve Cracking)

Table 4: Test Results of GFRP Sleeve Splice Specimens

Specimens ID	d_b (mm)	L_d* (mm)	Tensile capacity (kN)	Ultimate tensile stress (MPa)	Tensile strength (%)**	Bond strength (MPa)	Failure mode
G12-NW-13.75	12	165	62	548	50.7	9.96	Sleeve cracking
G12-2W-13.75		165	66	584	54.1	10.61	
G12-4W-13.75		165	72	637	58.9	11.57	
G12-NW-16.25		195	80	708	65.5	12.86	
G12-2W-16.25		195	85	752	69.6	13.66	
G12-4W-16.25		195	92	814	75.3	14.79	

* Embedment length of the GFRP bar in the sleeve connector

**Compared to the control specimen

4. Conclusions and Recommendations

This study proposed an alternative method to connect precast concrete elements by splice GFRP bars end-to-end in a GFRP sleeve filled with epoxy resin in order to make the connection smaller and durable. The behavior of GFRP sleeve splice bars under tension is investigated considering the bar embedment length and the number of GFRP layers confinement the GFRP sleeve. Based on test results, the following conclusions are drawn:

- The test results showed that the tensile capacity increased by increasing radial stiffness of the sleeve using higher number of wrapping GFRP layers. Specimen with four GFRP wrapping layers increased tensile capacity by 16% and 15% compared to specimen without wrapping for 13.75Ø and 16.25Ø embedment lengths, respectively.
- Sleeve cracking failure mode indicated that the radial stiffness of the GFRP sleeve is inadequate and additional confinement is needed as failure is not controlled by bond strength yet.
- The tensile capacity increased by increasing bar embedment length. Increasing the embedment length from 13.75 to 16.25 times bar diameter increased the tensile capacity by 29%, 37%, and 48% for specimens with no wrap, 2 and 4 layers, respectively.
- To produce a sleeve splice that achieves the required bar tensile strength, it should provide adequate radial stiffness to prevent the sleeve from cracking and adequate bar embedment length to prevent failure accrued due to bar slip controlled by bond stress capacity.
- Due to the lack of possibilities in the laboratory, future studies are needed to fabricate GFRP sleeves in plants with an adequate radial stiffness.

5. References

[1] ASTM, “Standard test method for tensile properties of fiber reinforced polymer matrix composite bars,” *ASTM D7205-11*, 2011.

[2] P. Hamill, M. Bertolini, H. Wilden, and M. Biebighauser, “Precast Concrete Value Engineering Accommodates Difficult Site,” *PCI J.*, vol. 51, no. 4, p. 18, 2006.

[3] S. Kale, D. Arditi, S. Kale, and D. Arditi, “Diffusion of ISO 9000 certification in the precast concrete industry,” *Constr. Manag. Econ.*, vol. 24, no. 5, pp. 485–495, 2006.

[4] J. D. Manrique, M. Al-hussein, A. Telyas, and G. Funston, “Case study-based challenges of quality concrete finishing for architecturally complex structures,” *J. Constr. Eng. Manag.*, vol. 133, no. 3, pp. 208–216, 2007.

[5] R. Soetanto, J. Glass, A. R. J. Dainty, and A. D. F. Price, “Structural frame selection: case studies of hybrid concrete frames,” *Build. Res. Inf.*, vol. 35, no. 2, pp. 206–219, 2007.

[6] W. T. Chan and H. Hu, “Constraint programming approach to precast production scheduling,” *J. Constr. Eng. Manag.*, vol. 128, no. 6, pp. 513–521, 2002.

[7] G. Eastman, C., Sacks, R., & Lee, “Development and implementation of advanced IT in the North American precast concrete industry,” *J. Inf. Technol. Constr.*, vol. 8, no. 18, pp. 247–262, 2003.

[8] R. Sacks, C. M. Eastman, and G. Lee, “Process model

perspectives on management and engineering procedures in the precast/prestressed concrete industry," *J. Constr. Eng. Manag.*, vol. 130, no. 2, pp. 206–215, 2004.

[9] S. J. A. Hosseinl and A. B. Ahmad, "Analysis of spiral reinforcement in grouted pipe splice connectors," *Gradjevinar*, vol. 65, no. 6, pp. 537–546, 2013.

[10] J. Ling and I. S. Ibrahim, "Tensile Performance of Modified Hollow Section Splice Sleeve Connector Under Direct Tensile Load," *Ciraic 2009*, 2009.

[11] A. A. Sayadi, A. B. A. Rahman, M. Z. Bin Jumaat, U. Johnson Alengaram, and S. Ahmad, "The relationship between interlocking mechanism and bond strength in elastic and inelastic segment of splice sleeve," *Constr. Build. Mater.*, vol. 55, pp. 227–237, 2014.

[12] J. H. Ling, A. B. Ahmad, I. S. Ibrahim, and Z. Abdul Hamid, "Behaviour of grouted pipe splice under incremental tensile load," *Constr. Build. Mater.*, vol. 33, pp. 90–98, 2012.

[13] A. J. Tibbetts, M. G. Oliva, and L. C. Bank, "Durable fiber reinforced polymer bar splice connections for precast concrete structures," *Compos. ploycon*, pp. 15–17, 2009.

[14] K. Koushfar, A. B. A. Rahman, Y. Ahmad, and M. H. Osman, "Bond behavior of the reinforcement bar in glass fiber-reinforced polymer connector," *Gradjevinar*, vol. 66, no. 4, pp. 301–310, 2014.

[15] A. A. Sayadi, A. B. Ahmad, A. Sayadi, M. Bahmani, and L. Shahryari, "Effective of elastic and inelastic zone on behavior of glass fiber reinforced polymer splice sleeve," *Constr. Build. Mater.*, vol. 80, pp. 38–47, 2015.

[16] C. Zhao, Z. Zhang, J. Wang, and B. Wang, "Numerical and theoretical analysis on the mechanical properties of improved CP-GFRP splice sleeve," *Thin Walled Struct.*, vol. 137, pp. 487–501, 2019.